INTERNATIONAL JOURNAL OF
NUMERICAL ANALYSIS AND MODELING, *SERIES B*
Volume 4, Number 1, Pages 1–13

A DIRECTION SPLITTING APPROACH FOR INCOMPRESSIBLE BRINKMAN FLOW

T. GORNAK, J.L. GUERMOND, O. ILIEV, AND P.D. MINEV

Abstract. The direction splitting approach proposed earlier in [7], aiming at the efficient solution of Navier-Stokes equations, is extended and adopted here to solve the Navier-Stokes-Brinkman equations describing incompressible flows in pure fluid and in porous media. The resulting pressure equation is a perturbation of the incompressibility constraint using a direction-wise factorized operator as proposed in [7]. We prove that this approach is unconditionally stable for the unsteady Navier-Stokes-Brinkman problem. We also provide numerical illustrations of the method's accuracy and efficiency.

Key words. Direction splitting, Navier-Stokes-Brinkman equations

1. Introduction

Flows in highly porous media occur often in industrial and scientific applications. Examples are the flows through various filters (air, oil, water filters, etc.), flow of helium in pebble-bed nuclear reactors, various physiological flows like the flow in the eye of glaucoma patients, flows in mangrove swamps etc. If the porosity of the media is high, such flows are usually modelled by the Navier-Stokes-Brinkman equations. These equations include as limiting cases the Darcy model for the flow in porous media with a very low porosity, and the Navier-Stokes equations for flows with infinitely large porosity. As in the case of the classical Navier-Stokes equations, one of the major computational problems for any discretization algorithm is the imposition of the incompressibility constraint. In the case of unsteady flows probably the most popular and efficient algorithms for the imposition of incompressibility are the so-called projection methods. These methods were pioneered by Chorin [4] and Temam [14][1]. For a recent and comprehensive review on projection methods the reader is referred to [6]. All projection methods are semi-discretizations of singular perturbation of the time-dependent Stokes equations where the continuity equation is perturbed. This perturbation yields a Poisson equation for the pressure or some correction thereof with Neumann boundary condition (L^2 projection onto a divergence-free subspace of the velocity space). The solution of this Poisson equation can often be a very computationally intensive task. To circumvent this difficulty [7] proposed to use a perturbation of the continuity equation based on a direction-wise factorized operator instead of the classical Laplace operator which allows for the use of a fast tri-diagonal direct solver. In the present article we extend this approach to the case of incompressible Navier-Stokes-Brinkman flow and demonstrate numerically that it produces results of the same accuracy as the classical projection methods. We also prove that if the momentum equation is not split direction-wise, the resulting algorithm is unconditionally stable.

Received by the editors October 16, 2012, and in revised form, February 12, 2013 .
2000 *Mathematics Subject Classification.* 65N30, 65N35.

[1]The authors have recently discovered that a similar velocity-pressure decoupling approach was proposed earlier in the famous article of Harlow and Welch [9] which also proposed the MAC staggered grid setting for the Stokes problem with free boundaries. Thus, we think some credit for pioneering the projection methods should be given to this article as well.

2. The fictitious domain Brinkman equations

Consider the Brinkman equations in a domain $\tilde{\Omega} \subset \mathbb{R}^d (d = 2, 3)$ with a Lipschitz boundary $\Gamma = \partial\tilde{\Omega}$:

$$\begin{cases} \partial_t \tilde{\mathbf{u}} - \tilde{\nu}\Delta\tilde{\mathbf{u}} + \nabla\tilde{p} + \dfrac{\tilde{\nu}}{\tilde{k}}\tilde{\mathbf{u}} = \tilde{\mathbf{f}} \quad \text{in } \tilde{\Omega} \times [0,T], \\ \nabla\cdot\tilde{\mathbf{u}} = 0 \quad \text{in } \tilde{\Omega} \times [0,T], \\ \tilde{\mathbf{u}}|_{\partial\tilde{\Omega}} = 0 \quad \text{in}[0,T], \quad \text{and } \tilde{\mathbf{u}}|_{t=0} = \tilde{\mathbf{u}}_0 \quad \text{in} \quad \tilde{\Omega}, \end{cases} \tag{1}$$

where $\tilde{\nu}$ is the kinematic viscosity of the fluid and $\tilde{k}$ is the permeability, and T is the final time moment. In order to use the direction-splitting algorithm proposed in [7] it is necessary to extend the domain of the problem to a simple rectangle/parallelepiped (in 2D/3D). Let Ω be be such an extension i.e. $\tilde{\Omega} \subseteq \Omega$ and consider the following extension of the data

$$\nu = \tilde{\nu}, \quad \text{in} \quad \Omega, \tag{2}$$

$$\mathbf{f} = \begin{cases} \tilde{\mathbf{f}}, & \text{in} \quad \tilde{\Omega}, \\ 0, & \text{in} \quad \Omega \setminus \tilde{\Omega}, \end{cases} \tag{3}$$

$$\mathbf{u}_0 = \begin{cases} \tilde{\mathbf{u}}_0, & \text{in} \quad \tilde{\Omega}, \\ 0, & \text{in} \quad \Omega \setminus \tilde{\Omega}, \end{cases} \tag{4}$$

$$k(\mathbf{x}) = \begin{cases} \tilde{k}, & \text{in} \quad \tilde{\Omega}, \\ \nu\epsilon, & \text{in} \quad \Omega \setminus \tilde{\Omega}, \end{cases} \tag{5}$$

where $0 < \epsilon << 1$ is a penalty parameter used to enforce the boundary conditions on $\partial\tilde{\Omega}$. Then the L^2-penalty fictitious domain formulation of the problem in Ω reads

$$\begin{aligned} &\partial_t \mathbf{u}_\varepsilon - \nu\Delta\mathbf{u}_\varepsilon + \nabla p_\varepsilon + \frac{\nu}{k}\mathbf{u}_\varepsilon = \mathbf{f}, \ x \in \Omega \times [0,T] \\ &\nabla\cdot\mathbf{u}_\varepsilon = 0 \text{ in } \Omega \times [0,T], \\ &\mathbf{u}_\varepsilon|_{\partial\Omega} = 0 \text{ in } [0,T], \text{ and } \mathbf{u}_\varepsilon|_{t=0} = \mathbf{u}_0 \text{ in } \Omega. \end{aligned} \tag{6}$$

It is well known (see for example [2]) that the following result holds under sufficient regularity assumptions on the data and the domain:

$$\mathbf{u}_\varepsilon \xrightarrow[\varepsilon\to 0]{} \tilde{\mathbf{u}}, \quad \text{in } L^2(\tilde{\Omega}\times(0,T)).$$

The order of convergence depends on the regularity of the data and the domain, but it is at least $O(\epsilon^{1/2})$.

3. Numerical algorithm

3.1. Time discretization. As we mentioned in the introduction, if the domain of the problem has a simple shape, it is convenient to perturb the continuity equation as follows: $\prod_{i=1}^{d} (I - \partial_{x_i x_i})\, \phi = -\nabla\cdot\mathbf{u}/\Delta t$ where ϕ is either the pressure itself (for first order schemes) or its time increment (for higher order schemes). Therefore, it would be also convenient to apply the same direction-splitting procedure to the momentum equation. However, since the permeability is space-dependent, the direction splitting of the momentum equation, in case of an implicit treatment of the Brinkman term $\nu\mathbf{u}_\varepsilon/k$, is not straightforward. To understand the problem, let us

consider the Douglas splitting for the first equation in (6) (see [10]) in the following factorized form

$$\prod_{i=1}^{d}\left(b(\mathbf{x})I-\frac{\nu\Delta t}{2b(\mathbf{x})}\partial_{x_ix_i}\right)\frac{\mathbf{u}^{n+1}-\mathbf{u}^n}{\Delta t}-\nu\Delta\mathbf{u}^n+\frac{\nu}{k}\mathbf{u}^n+\nabla p^{*,n+1/2}=\mathbf{f}^{n+1/2}, \tag{7}$$

where $b(\mathbf{x})=(1+\nu\Delta t/(2k(\mathbf{x})))^{1/d}$ and I is the identity operator. Since $b(\mathbf{x})^{-1}\partial_{x_1x_1}$ and $b(\mathbf{x})^{-1}\partial_{x_2x_2}$ do not commute in general, the operator product $b(\mathbf{x})^{-1}\partial_{x_1x_1}b(\mathbf{x})^{-1}\partial_{x_2x_2}$ is not necessarily positive and self-adjoint. Loss of positivity and self-adjointness affects the stability of the scheme. As proven in [13], section 2.2.3, in case of non-commutative splitting the Douglas scheme is unconditionally stable in 2D, but the stability in 3D cannot be guaranteed. Therefore, in this paper we do not consider the possibility to split direction-wise the momentum equation. As a result, the full 2D/3D momentum problem is solved by means of an iterative procedure. The reader is referred to [3] for some possibilities for a direction splitting of the momentum equation in the non-commutative case, however, no theory for the case of Navier-Stokes-Brinkman flows has been developed yet.

In the sequel of the paper we will omit the subscript ε for the solution of the penalized problem (6), and abusing somewhat the notation we will denote the solution of the semi-discrete (in time only) splitting scheme by $\mathbf{u}$ and p. Let us denote by p^0 the exact pressure field at $t=0$, and by $\phi^{-1/2}$ an approximation to $\Delta t\partial_t p(0)$. The initial pressure p^0 is not part of the initial data but it can be computed from $\Delta p^0=\nabla\cdot(\mathbf{f}_0+\Delta\mathbf{u}_0)$, $\partial_n p^0_{|\partial\Omega}=(\mathbf{f}_0+\Delta\mathbf{u}_0)\cdot\mathbf{n}$ under certain compatibility conditions on the data (see section 2.3 of [5]). The approximation $\phi^{-1/2}$ can then be computed using a non-incremental scheme at the first time step. Then setting $p^{-1/2}=p^0$ the scheme proceeds as follows for all $n\geq 0$:

Pressure predictor:

$$p^{*,n+1/2}=p^{n-1/2}+\phi^{n-1/2}. \tag{8}$$

Velocity update:

$$\begin{aligned}&\frac{\mathbf{u}^{n+1}-\mathbf{u}^n}{\Delta t}-\frac{1}{2}\nu\Delta(\mathbf{u}^{n+1}+\mathbf{u}^n)+\nabla p^{*,n+1/2}+\\&\frac{\nu}{2k}(\mathbf{u}^{n+1}+\mathbf{u}^n)=\mathbf{f}^{n+1/2},\qquad \mathbf{u}^{n+1}|_{\partial\Omega}=\mathbf{0}.\end{aligned} \tag{9}$$

Pressure-corrector:

$$A\phi^{n+1/2}=-\tfrac{1}{\Delta t}\nabla\cdot\mathbf{u}^{n+1}, \tag{10}$$

where $A=\prod_{i=1}^{d}(I-\partial_{x_ix_i})$ together with homogeneous Neumann boundary conditions on $\partial\Omega$. Note that this operator is factorized alongside the spatial directions and is therefore much easier to invert than the usual Laplace operator. The bilinear form $a(p,q):=\int_\Omega qAp\mathrm{d}\mathbf{x}$ satisfies the following properties (see [7]):

$$a \text{ is symmetric,} \qquad \text{and} \qquad \|\nabla q\|^2_{\mathbf{L}^2}\leq a(q,q),\quad \forall q\in D(A). \tag{11}$$

where $D(A)$ is the domain of A.

Pressure update:

$$p^{n+1/2}=p^{n-1/2}+\phi^{n+1/2}-\frac{1}{2}\chi\nu\nabla\cdot(\mathbf{u}^{n+1}+\mathbf{u}^n), \tag{12}$$

where $\chi\in[0,1]$.

The stability of the scheme is guaranteed by the following theorem.

Theorem 3.1. *Assume that the solution to* (6) *is smooth enough. For all T, there exist c, independent of Δt, such that for all $\chi \in [0,1]$ the solution to (8)-(10) and (12), satisfies the following stability estimate:*

$$
\begin{aligned}
&\|\boldsymbol{u}\|^2_{\ell^\infty(0,T;\boldsymbol{L}^2)} + \frac{\Delta t}{2}\|\nu^{1/2}\nabla\boldsymbol{u}\|^2_{\ell^\infty(\Delta t,T;\boldsymbol{L}^2)} + \Delta t^2\|p\|_{\ell^\infty(\frac{\Delta t}{2},T-\frac{\Delta t}{2},D(A))} + \\
&\frac{\Delta t}{2}\|\left(\frac{\nu}{k}\right)^{1/2}\boldsymbol{u}\|^2_{\ell^\infty(\Delta t,T;\boldsymbol{L}^2)} \le c(\|\boldsymbol{u}^0\|^2_{\boldsymbol{L}^2} + \Delta t^2\|p^{-1/2}\|^2_A + \\
&\frac{\Delta t}{2}\|\nu^{1/2}\nabla\boldsymbol{u}^0\|^2_{\boldsymbol{L}^2} + \frac{\Delta t}{2}\|\left(\frac{\nu}{k}\right)^{1/2}\boldsymbol{u}^0\|^2_{\boldsymbol{L}^2} + \nu^{-1}\|\mathbf{f}\|_{\ell^2(\frac{\Delta t}{2},T-\frac{\Delta t}{2};\boldsymbol{H}^{-1})}).
\end{aligned}
\tag{13}
$$

Proof. The proof proceeds along the same lines as in [7]. Nevertheless, there are some minor differences and we provide a brief sketch here for the case $\chi = 0$ and $\mathbf{f} = \mathbf{0}$ only. This stability estimate can then be used to estimate the accuracy of the scheme by proceeding as in [8]. We first multiply (9) by $2\Delta t\mathbf{u}^{n+1}$, integrate over Ω, and use the identity $2(a-b,a) = \|a\|^2 + \|a-b\|^2 - \|b\|^2$ and the Young's inequality to obtain

$$
\begin{aligned}
&\|\mathbf{u}^{n+1}\|^2_{\mathbf{L}^2} + \|\mathbf{u}^{n+1}-\mathbf{u}^n\|^2_{\mathbf{L}^2} + \frac{\Delta t}{2}\|\nu^{1/2}\nabla\mathbf{u}^{n+1}\|^2_{\mathbf{L}^2} \\
&+ 2\Delta t(\nabla p^{*,n+1/2},\mathbf{u}^{n+1}) + \frac{\Delta t}{2}\|\left(\frac{\nu}{k}\right)^{1/2}\mathbf{u}^{n+1}\|^2_{\mathbf{L}^2} \le \\
&\|\mathbf{u}^n\|^2_{\mathbf{L}^2} + \frac{\Delta t}{2}\|\nu^{1/2}\nabla\mathbf{u}^n\|^2_{\mathbf{L}^2} + \frac{\Delta t}{2}\|\left(\frac{\nu}{k}\right)^{1/2}\mathbf{u}^n\|^2_{\mathbf{L}^2}.
\end{aligned}
\tag{14}
$$

Now we use the properties (11) to deduce that the pressure correction $(p^{n+1/2} - p^{n-1/2}) \in D(A)$ solves the following problem for $n \ge 0$:

$$
a(p^{n+1/2}-p^{n-1/2},q) = -\Delta t^{-1}(\nabla\cdot\mathbf{u}^{n+1},q), \qquad \forall q \in D(A).
\tag{15}
$$

Testing this equation with $2\Delta t^2 p^{*,n+1/2} := 2\Delta t^2(2p^{n-1/2} - p^{n-\frac{3}{2}})$ (in case $\chi = 0$) and using the symmetry and coercivity of $a(\cdot,\cdot)$, exactly as in the proof of Theorem 4.2 in [7], we obtain that

$$
\begin{aligned}
-2\Delta t(\nabla\cdot\mathbf{u}^{n+1},p^{*,n+1/2}) = \Delta t^2\Big(&\|p^{n+1/2}\|^2_A - \\
&\|p^{n-1/2}\|^2_A + \|\delta p^{n-1/2}\|^2_A - \|\delta^2 p^{n+1/2}\|^2_A\Big).
\end{aligned}
\tag{16}
$$

where $\delta p^{n-1/2} = p^{n-1/2} - p^{n-3/2}$ is the usual difference operator. Again as in the proof of Theorem 4.2 in [7], the control on $\|\delta^2 p^{n+1/2}\|^2_A$ is obtained subtracting (15) at time t^n from (15) at time t^{n+1} and by testing the result with $\Delta t\delta^2 p^{n+1/2}$,

$$
\begin{aligned}
\Delta t\|\delta^2 p^{n+1/2}\|^2_A &= -(\nabla\cdot(\mathbf{u}^{n+1}-\mathbf{u}^n),\delta^2 p^{n+1/2}) = (\mathbf{u}^{n+1}-\mathbf{u}^n,\nabla\delta^2 p^{n+1/2}) \\
&\le \|\mathbf{u}^{n+1}-\mathbf{u}^n\|_{\mathbf{L}^2}\|\nabla\delta^2 p^{n+1/2}\|_{\mathbf{L}^2}.
\end{aligned}
$$

Then the coercivity property of the bilinear form a implies that

$$
\Delta t\|\nabla\delta^2 p^{n+1/2}\|_{\mathbf{L}^2}\|\delta^2 p^{n+1/2}\|_A \le \|\mathbf{u}^{n+1}-\mathbf{u}^n\|_{\mathbf{L}^2}\|\nabla\delta^2 p^{n+1/2}\|_{\mathbf{L}^2},
$$

which yields the inequality $\Delta t^2\|\delta^2 p^{n+1/2}\|^2_A \le \|\mathbf{u}^{n+1}-\mathbf{u}^n\|^2_{\mathbf{L}^2}$. This bound together with (16) gives the following bound on the pressure gradient term in (14)

$$
\begin{aligned}
\Delta t^2\Big(&\|p^{n+1/2}\|^2_A + \|\delta p^{n-1/2}\|^2_A - \|p^{n-1/2}\|^2_A\Big) \le \\
&-2\Delta t(\nabla\cdot\mathbf{u}^{n+1},p^{*,n+1/2}) + \|\mathbf{u}^{n+1}-\mathbf{u}^n\|^2_{\mathbf{L}^2}
\end{aligned}
\tag{17}
$$

which after summing with (14) gives

$$\|\mathbf{u}^{n+1}\|^2_{\mathbf{L}^2} + \Delta t^2 \|p^{n+1/2}\|^2_A + \frac{\Delta t}{2}(\|\nu^{1/2}\nabla \mathbf{u}^{n+1}\|^2_{\mathbf{L}^2} + \frac{\Delta t}{2}\| \left(\frac{\nu}{k}\right)^{1/2} \mathbf{u}^{n+1}\|^2_{\mathbf{L}^2} \leq \|\mathbf{u}^{n}\|^2_{\mathbf{L}^2} + \Delta t^2 \|p^{n-1/2}\|^2_A + \frac{\Delta t}{2}\|\nu^{1/2}\nabla \mathbf{u}^{n}\|^2_{\mathbf{L}^2} + \frac{\Delta t}{2}\| \left(\frac{\nu}{k}\right)^{1/2} \mathbf{u}^{n}\|^2_{\mathbf{L}^2}. \tag{18}$$

The final estimate is obtained by summing (18) over the time levels from 0 to $N-1 = T/\Delta t - 1$. □

This stability estimate can be used to derive a first order error estimate on the velocity and the pressure in the L^2 norm as in theorem 3.1 of [5]. However, the main problem that prevents the derivation of an optimal second order estimate on the velocity in the fully split case of the Stokes equations considered in [5], remains in the present case too. In essence, it is due to the fact that the norm generated by the factorized operator A is not equivalent to the H^1 norm which in turn does not allow to apply the usual duality argument for obtaining an optimal estimate. So, in the present case, as in the case of the Stokes problem with split momentum equation considered in [5], using the same arguments, we can at present derive only that the velocity error in the L^2 norm is of order $\Delta t^{3/2}$ if $\chi > 0$. (see theorem 4.2 of [5]). The only improvement in the present case is that this result is valid irrespectively of the spatial dimension because the momentum equation is not discretized with a direction splitting scheme. Overall, the extension of all results for the Stokes problem in simple domains obtained in [5] to the Brinkman case is quite straightforward. The purpose of the present paper is mainly to show that the factorized perturbation of the incompressibility constraint (10) works in the Brinkman case independently of the domain shape, i.e., the pressure can be extended outside of the fluid domain with a penalty approach, and the resulting splitting scheme is stable.

3.2. Spatial discretization. The equations (9)–(10) and (12) are discretized in space using the classical MAC stencil (see [9], figure 1). When discretizing the momentum equation in complex-shaped domains in the case of a MAC grid, it is necessary to take special care for computing the Brinkman term, $\nu\mathbf{u}/k$, to preserve the accuracy. Essentially, such procedures compute some approximate or exact average of the coefficient ν/k over the MAC cells intersected by a boundary marking a jump in this quantity (see for example [12], section 3.2).

The conservative finite volume approximation of the second derivative in the x-direction on a grid of a nonuniform grid size h_i is given by

$$D_x u^n_{i,j,k} = \frac{2}{h_{i+1}+h_i}\left(\bar{\nu}_{i-1/2}\frac{u^n_{i,j,k}-u^n_{i-1,j,k}}{h_i} - \bar{\nu}_{i+1/2}\frac{u^n_{i+1,j,k}-u^n_{i,j,k}}{h_{i+1}}\right), \tag{19}$$

where

$$\bar{\nu}_{i-1/2} = \left(\int_{-1}^{0} \frac{ds}{\nu(x_i + sh_i, y, z)}\right)^{-1} \tag{20}$$

is the average of ν on $[x_{i,j,k}, x_{i-1,j,k}]$, and $h_i = x_{i,j,k} - x_{i-1,j,k}, \quad i = 2, \ldots, L$. Note that if the integral in (20) is approximated by means of a trapezoid quadrature, $\bar{\nu}$ would be equal to the harmonic average of ν over a given discretization cell. This discretization can be used to compute the central difference in any of the spatial directions in case of variable viscosity.

Similarly, the average Brinkman porosity at the point with x-coordinate x_i can be computed as:

$$\bar{k}_i = \left(\int_0^1 \frac{ds}{k(x_{i-1/2} + 0.5s(h_i + h_{i+1}), y, z)} \right)^{-1} \tag{21}$$

An alternative spatial approximation is provided by the stabilized central difference discretization on a collocated grid for the velocity and pressure proposed by Rhie and Chow [11]. All the test cases presented in the next section were also computed using such a collocated approximation and the results (not reported here) showed a very similar behavior as the one computed on the MAC grid (presented below).

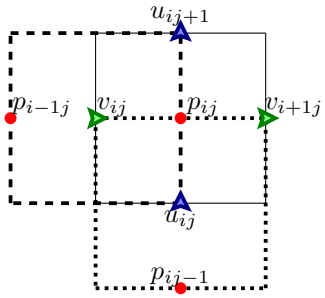

FIGURE 1. Control volumes associated with each node in case of MAC grid

3.3. Computational cost of the direction splitting operator vs. Laplace operator in the pressure correction equation. For simplicity, let us consider a cubic domain covered with a grid containing $n \times n \times n$ nodes. Under the assumption that the cost for assembling the matrices is small compared to the cost of solving the systems of linear equations, let us evaluate the number of operations needed for computing the solution for the pressure *per time step*.

Direction splitting operator. In 3D, the Thomas algorithm for tri-diagonal matrices has to be employed $3n^2$ times (i.e., n^2 times in each direction). Each Thomas algorithm solve requires $5n$ multiplications/divisions and $3n$ summations/subtractions. So, the total of $15n^3 + 9n^3$ operations are required.

Laplace operator. Suppose now that we use an iterative method to solve the pressure Poisson equation[2]. Each iteration requires at least one matrix-vector multiplication, which for a seven-diagonal matrix will require $7n^3$ multiplications and $6n^3$ summations, thereby $7n^3 + 6n^3$ is the total number of operation for one single matrix-vector multiplication.

The above operation count shows that even if the iterative method converges within several iterations, the solution of pressure equation with a direction splitting operator and a direct tri-diagonal solver requires less operations than the iterative solution of the pressure Poisson equation.

[2]Note that the Poisson equation can be solved using fast Fourier transform (FFT). The parallel performance of the FFT algorithm, however, is not as good as that of a Thomas-based Schur complement approach (see [7])

4. Simulations

4.1. Preliminaries. The performance of the two approximations to the incompressibility constraint discussed here: the pressure Poisson equation, and the directionally factorized perturbation (10), is compared on two two-dimensional problems involving fluid and porous regions. The domain of the first problem is a channel with sudden contraction, containing a subdomain (called here porous subdomain) with a given permeability. If the permeability is very large, the Darcy term in the Brinkman equations tends to zero, and therefore the flow in the porous subdomain is unrestricted similarly to the rest of the fluid domain. For very small values of the permeability, the Darcy term dominates in the porous subdomain, and completely prevents the flow through it. In fact, in this case the Stokes-Brinkman equations become a Fictitious Domain (penalty) formulation for the Stokes equations with no-slip boundary conditions on the boundary of the subdomain in which an extremely low porosity is defined. The domain of the second problem is a channel with two porous subdomains. In this case time dependent boundary conditions are applied.

The main goal of these simulations is to compare the results for the velocity and pressure computed with the classical Poisson equation for the pressure increment (classical incremental projection scheme in a rotational form; see [6]), and the factorized operator A defined above. Therefore, we define $\mathbf{u}_\Delta, p_\Delta$ to be the velocity and pressure calculated using the classical projection scheme, and $\mathbf{u}_A, p_A$ – the velocity and pressure calculated using the scheme with the operator A in the pressure correction step.

In all test cases presented below the viscosity is set to be $\nu = 10^{-6} m^2 \cdot s^{-1}$ and the parameter χ is set to one. The momentum equation of both schemes and the pressure-Poisson equation in the classical projection scheme are solved by a generalized minimal residual method with ILU preconditioner (see [1] for implementation details). All simulations were performed on a machine with a dual core Intel Xeon 5148LV with 8 GB RAM .

4.2. Flow in a channel with a sudden contraction and a porous obstacle. As a first test case, consider the flow in a channel with a sudden contraction and a porous obstacle (see figure 2). No-slip boundary conditions are prescribed on the entire boundary except for the the inlet AB and the outlet CD where a parabolic profile for the velocity is prescribed:

$$\begin{aligned} u_{AB} = &\quad \alpha_1 x_1 (x_1 - 1.5), \quad 0 \le x_1 \le 1.5, \quad x_2 = 3 \\ u_{CD} = &\quad \alpha_2 x_1 (x_1 - 0.6), \quad 0 \le x_1 \le 0.6, \quad x_2 = 0 \end{aligned}$$

The coefficients α_1 and α_2 are specified so that the flow rates at both ends of the channel are equal:

$$\int_0^{1.5} \alpha_1 x (x - 1.5) dx = \int_0^{0.6} \alpha_2 x (x - 0.6) dx = 0.015.$$

The usual zero Neumann boundary condition on the entire boundary is imposed on the pressure correction.

We show in figure 3 the L^2 norm of the difference of the velocities and pressures, $\|u_\Delta - u_A\|_{L_2}$ and $\|p_\Delta - p_A\|_{L_2}$, as a function of Δt. The convergence rate of both errors is similar to the theoretical estimates for the convergence error of the classical incremental projection scheme in a rotational form (see [8]): second order for the velocity and order 3/2 for the pressure error in the L^2 norm. At the same time, the

simulations with the directional splitting approach (using the factorized operator A) are significantly faster (see table 1).

To compare the CPU time usage we must take into account that the computational time for iterative solvers depends on the number of iterations, which in turn depends on the preset tolerance of the solver and the time step. All this information is summarized in table 1.

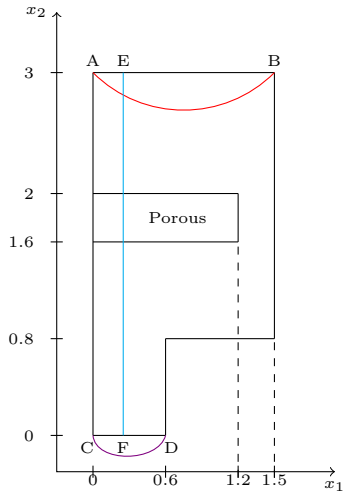

FIGURE 2. Sketch of a channel with a sudden contraction and a porous obstacle.

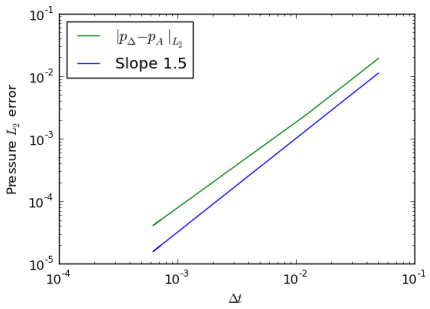

(A) Pressure L^2 error: $\|p_\Delta - p_A\|_{L_2}$

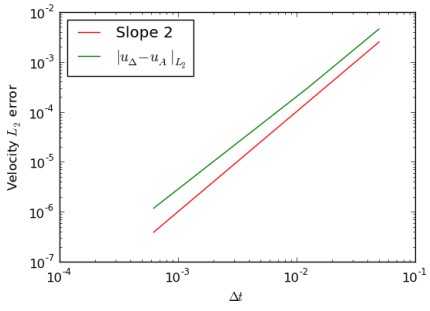

(B) Velocity L^2 error: $\|u_\Delta - u_A\|_{L_2}$

FIGURE 3. Pressure and velocity error; test case of section 4.2 ($h = 0.005$).

In the left panel of figure 4 we present the horizontal profiles of the velocity along the vertical segment EF (see figure 2) at various permeabilities. The corresponding velocity vectors are displayed in the right panel of figure 4.

TABLE 1. CPU time comparison; test case of section 4.2

h/N	Δt	Tolerance for iterative solver	Time for Laplace	Time for DS operator	Speed up
0.01/37800	1e-5	1e-8	18.18	2.35	7.7
0.01/37800	1e-5	1e-12	34.12	2.35	14.52
0.01/37800	1e-7	1e-8	22.14	2.35	9.42
0.01/37800	1e-7	1e-12	28.89	2.35	12.3
0.005/151200	1e-5	1e-8	86.12	6.57	13.1
0.005/151200	1e-5	1e-12	97.43	6.57	14.8
0.005/151200	1e-7	1e-8	78.16	6.57	11.8
0.005/151200	1e-7	1e-12	84.25	6.57	12.8

4.3. Flow in a channel with two porous obstacles and time dependent boundary conditions. To further illustrate the properties of the factorized scheme, consider the flow in a vertical channel with two porous blocks (see figure 5). No-slip boundary conditions are prescribed on the solid walls AC and BD, while at the inlet AB and the outlet CD a time dependent profile for the velocity is prescribed: $-(\pi + \sin(5t))$. The domain is given by: $0 \leq x_1 \leq 1.5$, $0 \leq x_2 \leq 1$.

In figure 6 we show the norm of the difference of the velocities and the pressures, $\|u_\Delta - u_A\|_{L_2}$ and $\|p_\Delta - p_A\|_{L_2}$, as a function of Δt, and in figure 7, the vertical profiles of the velocity along the vertical segment EF, as well as the velocity vectors in the entire domain. As in the previous test case, the velocity and pressure difference has a very similar convergence rate to the corresponding convergence errors of the classical incremental projection scheme in a rotational form.

Table 2 shows the CPU time comparison for the two schemes, confirming again that the simulations with the direction splitting approach are significantly faster .

TABLE 2. CPU time comparison; test case of section 4.3.

h/N	Δt	Tolerance for iterative solver	Time for Laplace	Time for DS operator	Speed up
0.01/45000	1e-5	1e-8	20.24	2.4	8.61
0.01/45000	1e-5	1e-12	38.12	2.4	16.2
0.01/45000	1e-7	1e-8	27.14	2.4	11.54
0.01/45000	1e-7	1e-12	33.89	2.4	14.42
0.005/180000	1e-5	1e-8	88.15	6.8	12.9
0.005/180000	1e-5	1e-12	99.4	6.8	14.6
0.005/180000	1e-7	1e-8	79.25	6.8	11.6
0.005/180000	1e-7	1e-12	85.13	6.8	12.5

5. Conclusions

The results presented in this article demonstrate that the direction-factorized perturbation of the incompressibility constraint of the Stokes equations proposed

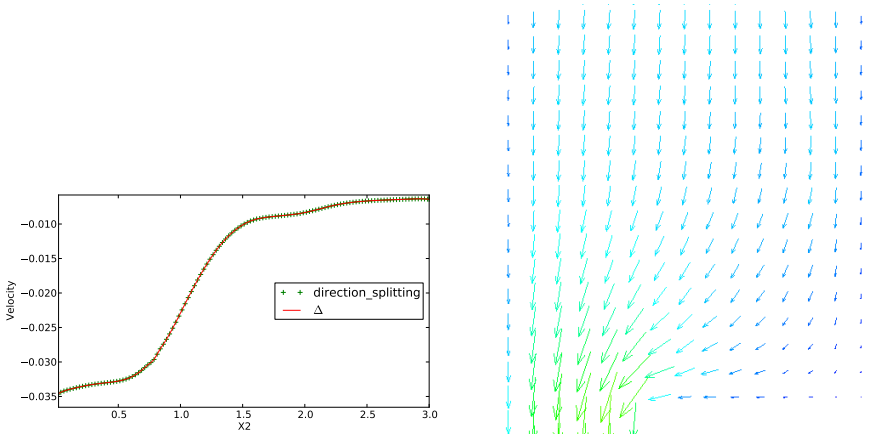

High permeability ($k = 10^{-4}$).

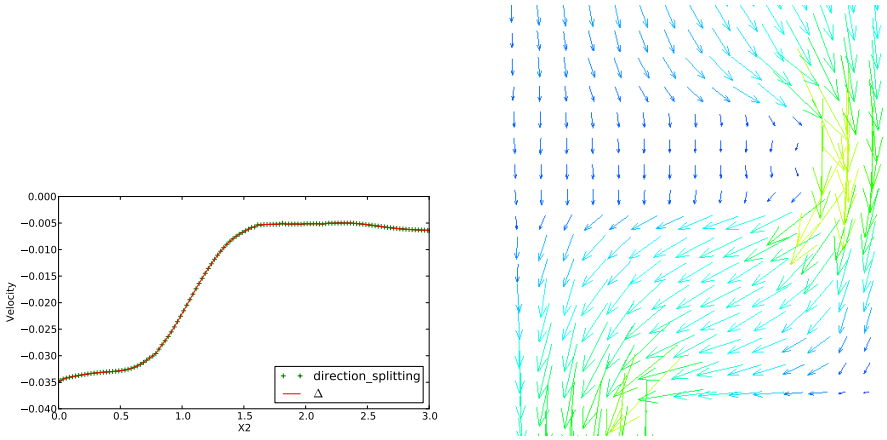

Moderate permeability ($k = 10^{-6}$).

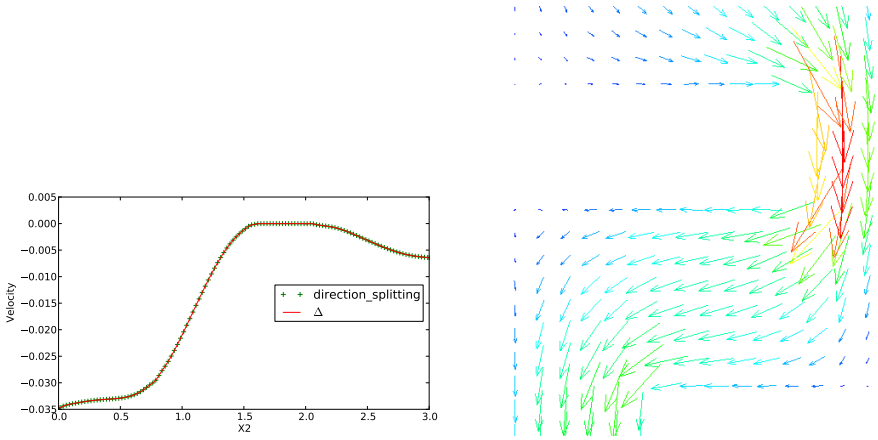

Extremely low permeability ($k = 10^{-8}$).

FIGURE 4. Velocity profile in the segment EF and the corresponding velocity field for different values of permeability; test case of section 4.2 ($h = 0.025, \Delta t = 0.01$).

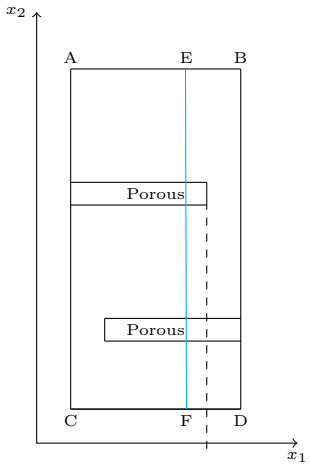

FIGURE 5. Sketch of the channel with two porous obstacles.

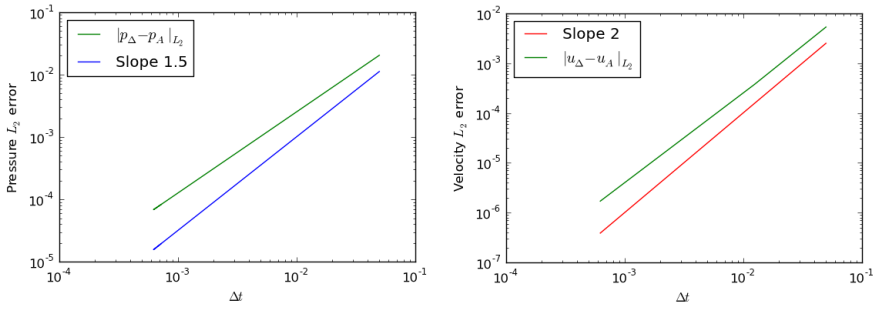

(A) Pressure L^2 error: $\|p_\Delta - p_A\|_{L_2}$

(B) Velocity L^2 error: $\|\mathbf{u_\Delta} - \mathbf{u_A}\|_{\mathbf{L_2}}$

FIGURE 6. Pressure and velocity error; test case of section 4.3 ($h = 0.005$).

in [7] can be applied to the Stokes-Brinkman equations. The scheme proposed in this paper is unconditionally stable. We have not considered the possibility for direction splitting of the momentum equations since it would generally yield non-commutative one-dimensional operators which significantly complicates the stability estimate. Although some possibilities for such splitting of the momentum equation in the non-commutative case are discussed in [3] the stability of the overall algorithm in the Stokes or Stokes-Brinkman case is still an open problem.

The numerical results presented in the paper on two test cases involving fluid and porous areas demonstrate that the L^2-norms of the differences between the velocities and pressures computed with the current direction-slitting approach and the classical incremental projection scheme in a rotational form behaves like $O(\Delta t^2)$ and $O(\Delta t^{3/2})$, respectively. In other words, the convergence rates in time of the two algorithms are close to the theoretical estimates for the incremental projection scheme in a rotational form.

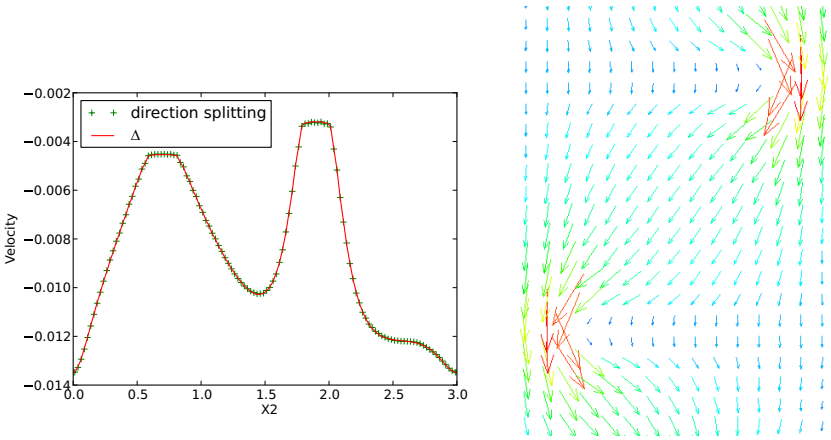

Moderate permeability in both porous areas ($k_{upper} = k_{lower} = 10^{-6}$).

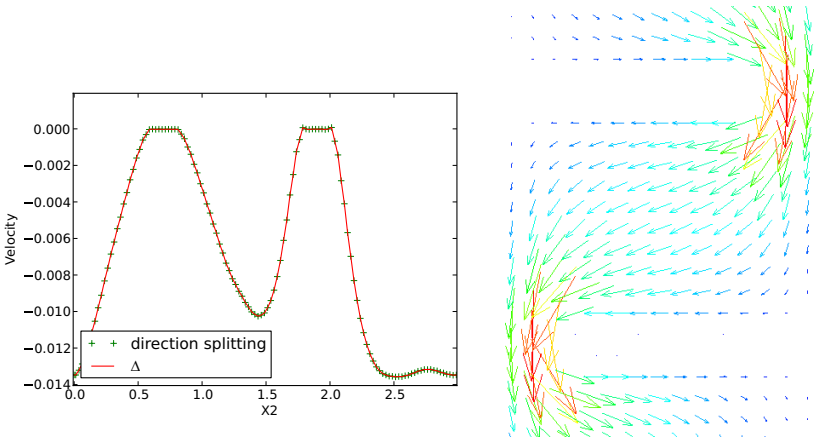

Low permeability in both porous areas ($k_{upper} = k_{lower} = 10^{-8}$).

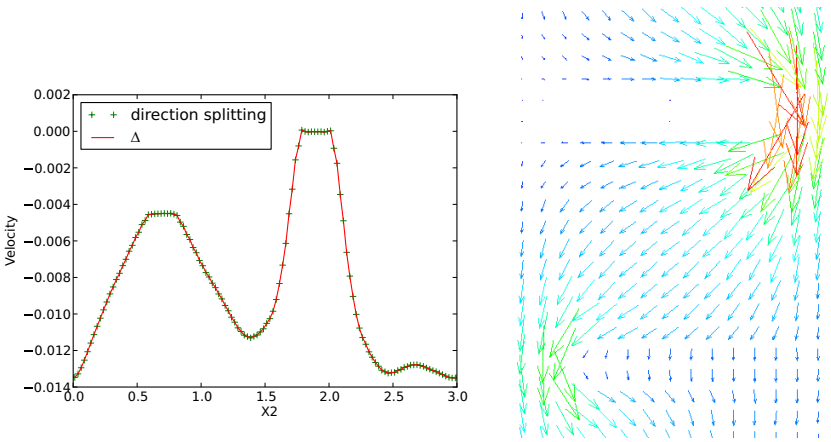

Low permeability in the upper area ($k_{upper} = 10^{-8}$), and moderate permeability in the lower area ($k_{lower} = 10^{-6}$)

FIGURE 7. Velocity in the slice and corresponding velocity vectors for different values of permeability; test case of section 4.3 ($h = 0.025, \Delta t = 0.01$)

Acknowledgments

The research of the first and the third authors (TG and OI) is supported by grant from German BMWi No. 11224. The second author (JLG) is partially supported by Award No. KUS -C1-016-04, made by King Abdullah University of Science and Technology (KAUST). The fourth author (PM) acknowledges the support of an NSERC Discovery grant and the support of ITWM, Kaiserslautern.

References

[1] Scipy v0.11.dev reference guide.
[2] Ph. Angot. Analysis of singular perturbations on the Brinkman problem for fictitious domain models of viscous flows. *Math. Meth. Applied Sciences*, 22(16):1395–1412, 1999.
[3] Ph. Angot, J. Keating, and P.D. Minev. A direction splitting algorithm for incompressible flow in complex geometries. *Comput. Methods Appl. Mech. Engrg.*, 217:111–120, 2012.
[4] A.J. Chorin. Numerical solution of the Navier-Stokes equations. *Math. Comp.*, 22:745–762, 1968.
[5] J.-L. Guermond, P. Minev, and A. Salgado. Convergence analysis of new class of direction splitting algorithm for the Navier-Stokes equations. *Math. Comp.*, 81(280):1951–1977, 2012.
[6] J.-L. Guermond, P. Minev, and J. Shen. An overview of projection methods for incompressible flows. *Comput. Methods Appl. Mech. Engrg.*, 195:6011–6054, 2006.
[7] J.-L. Guermond and P.D. Minev. A new class of splitting methods for the incompressible Navier-Stokes equations using direction splitting. *Comput. Methods Appl. Mech. Engrg.*, 200:2083–2093, 2011.
[8] J. L. Guermond and J. Shen. On the error estimates for the rotational pressure-correction projection methods. *Math. Comp.*, 73(248):1719–1737, 2004.
[9] F. Harlow and J.E. Welch. Numerical calculation of time-dependent viscous incompressible flow of fluid with a free surface. *Phys. Fluids*, 8(2):2182–2189, 1965.
[10] J. Douglas Jr. Alternating direction methods for three space variables. *Numer. Math.*, 4:41–63, 1962.
[11] C.M. Rhie and W.L. Chow. Numerical study of the turbulent flow past an airfoil with trailing edge separation. *AIAA J.*, 21:1525–1532, 1983.
[12] A. Samarskii. *The theory of difference schemes*. Marcel Dekker, Inc., 2001.
[13] A. Samarskii and A Vabishchevich. *Additive schemes for problems of Mathematical Physics (in Russian)*. Nauka, Moskva, 1999.
[14] R. Temam. Sur l'approximation de la solution des équations de Navier-Stokes par la méthode des pas fractionnaires ii. *Arch. Rat. Mech. Anal.*, 33:377–385, 1969.

Department of Flows and Materials Simulation Fraunhofer Institute for Industrial Mathematics, Fraunhofer-Platz 1, D-67663 Kaiserslautern, Germany and Technical University of Kaiserslautern, Kaiserslautern, Germany
E-mail: gornak@itwm.fhg.de

Department of Mathematics, Texas A&M University, College Station, TX 77843-3368, USA, and LIMSI (CNRS-UPR 3152), BP 133, 91403, Orsay, France
E-mail: guermond@math.tamu.edu

Department of Flows and Materials Simulation Fraunhofer Institute for Industrial Mathematics, Fraunhofer-Platz 1, D-67663 Kaiserslautern, Germany and Technical University of Kaiserslautern, Kaiserslautern, Germany and Inst. of Mathematics, Bulgarian Academy of Science, Sofia, Bulgaria
E-mail: iliev@itwm.fhg.de

Department of Mathematical and Statistical Sciences, University of Alberta, Edmonton, Alberta, Canada T6G 2G1
E-mail: minev@ualberta.ca